

**Colloidal Crystallization of Polymer-Grafted Silica
and Immobilization of Colloidal Crystals for
Optical Application**

ZhiGuo MA

Kyushu Institute of Technology

2011

Content

Chapter 1	1
Introduction.....	1
Reference	4
Chapter 2.....	7
Improvement of refractive index of colloidal crystals by incorporation of ferrocenyl group	7
2.1 Introduction.....	7
2.2 Experimental	9
2.3 Results and discussion	17
2.3.1 Grafting of poly(FcMA-MMA) with the colloidal silica.....	17
2.3.2 Colloidal crystallization	17
2.3.3 Effective refractive index.....	22
2.3.4 TEM observation of copolymer-grafted silica	27
2.4 Conclusions.....	- 29 -
2.5 References.....	- 30 -
Chapter 3.....	- 33 -
The disordering of particle-arrayed structure of colloidal crystals during immobilization	- 33 -
3.1 Introduction.....	- 33 -
3.2 Experiments	- 35 -
3.3 Result and discussion.....	- 38 -
3.3.1 Colloidal crystallization of PMMA-grafted silica	- 38 -
3.3.2 Immobilization of colloidal crystals	42
3.3.3 Single crystal size	44
3.3.4 Inter-sphere distance	46
3.4 Conclusions.....	49

3.5 References.....	50
Conclusion	52
Acknowledgements.....	53
Publication list	54

Chapter 1

Introduction

Recently, three-dimensional (3D) particle-arrayed structure, inter-particle space of which is comparable to visible light wave length, has been received great attention to application for optical devices, such as photonic crystal, wave guide, sensors, and so on [1–3]. In this regard, some practical methods for fabrication of 3D stereoregular structure, such as laser processing and photo- or electron- beamed lithographic techniques have been proposed [4-7]. Until now, however, there are no promising techniques for fabricating 3D particle-arrayed structure which are based on conventional and simple self-assembly of micro-particles in a colloidal suspension.

So far, many challenging approaches for preparation of polymeric materials contained of 3D particle-arrayed structure have been done by using colloidal inorganic particles [8, 9]. In this sense, colloidal crystallization, being a self-assembling phenomenon of colloidal particles to form crystal-like structure due to electrostatic repulsion, is one of promising procedures for fabrication of 3D particle-arrayed structure. Especially, colloidal silica has advantages for colloidal crystallization, because of easy available and high surface charge.

On overviewing previous studies, colloidal crystals are categorized into two types, hard type and soft type [10-17]. The hard-type colloidal crystals have advantage for making large size of single crystal [10-13], but are principally unfavorable for controlling inter-sphere distance to tune inter-sphere space. On the other hand, the soft-type colloidal crystals usually give sharp Bragg reflection peaks and has an advantage of ease changing inter-sphere distance with particle volume fraction, which is fairly attractive for application to photonic devices. For 3D particle-arrayed materials prepared by fabrication of colloidal crystals, Bragg reflection essentially depends on two factors: (1) the refractive index difference between particles and

suspension media, (2) space between spheres, i.e. lattice constant. Therefore, the reflection peaks reversibly change with these parameters by applying external stimuli, such as temperature, pH value, electric or magnetic fields, ion strength, and solvent composition [18-24], which exhibits potential application. Asher et al. immobilized the colloidal crystals for the first time and changed the lattice distance of colloidal crystals by pH and ionic strength [25]. Yamanaka et al. succeeded in constructing a photonic crystal system that covers a wide range of visible light by a mechanical stress gradient using polyacrylamide [26]. Takeoka and Watanabe made the preparation of structural-colored colloidal crystals that displays controlled multicolors by changing the composition of the mixed solvent [15]. Xia et al. fabricated 3D photonic crystal that operates in the visible regime from polystyrene in a controllable way by annealing the sample at elevated temperatures [27]. Also, Sawada et al. fabricated colloidal crystals that are incorporated in a polymer hydrogel matrix by the thermally induced unidirectional crystallization of colloidal silica in coexistence with pyridine [17]. Jiang et al. reported a compatible doctor blade coating technology for producing 3D highly ordered colloidal crystal-polymer nanocomposites, colloidal crystals, and macroporous polymer membranes [28]. Foulger et al. prepared stable polymer light-emitting diode (PLED) aqueous colloidal dispersions using π -conjugated emissive polymers to achieve color-tailored emissions spanning the visible spectrum [29].

Generally, for the application of colloidal crystals for optical devices, it is substantially required to immobilize colloidal crystals to fabricate 3D particle array structure. In most cases, the colloidal crystals are formed in aqueous media, and hydrogel is used to control and immobilize the colloidal crystal array [25, 30-36]. However, the hydrogels are sometimes inconvenient for practical application to photonic devices, because of containing much amount of water. In this respect, colloidal crystallization of polymer-grafted silica in organic solvents and immobilization into polymer matrix to prepare durable materials composed of 3D particle-arrayed structure have substantially synthetic merits, in terms of variety of organic reactions

[37-41]. Although, as described above, silica is a convenient and easy available material to fabricate 3D particle-arrayed structure through colloidal crystallization, a major problem for application of colloidal crystals of silica to photonic devices still remain; that is relatively low refractive index, $n=1.49$, and dielectric constant, $\epsilon \leq 2.5$, of silica. Moreover, optimization of immobilization condition of colloidal crystals formed in solution into polymer matrix is also much important to construct high performance 3D particle-arrayed materials.

This thesis describes incorporation of ferrocenyl group into colloidal crystals of polymer-grafted silica to make the refractive index of the system, and effects of particle volume fraction on disordering of 3D structure in colloidal crystals during immobilization.

In Chapter 1, background of the present research is reviewed.

In Chapter 2, colloidal crystallization of colloidal silica modified with copolymer of poly(ferrocenylmethyl methacrylate-*co*-methyl methacrylate) in organic solvent and effects of introduced ferrocenyl group to grafted polymer on effective refractive index (n_{eff}) of colloidal crystal system are described [42].

Chapter 3 describes investigation dependence of disordering of crystal-like structure in colloidal crystals on particle volume fraction through immobilization process by two-step radical polymerization [43].

References

1. Yablonovitch, E.; *Phys. Rev. Lett* 1987, 58, 2059.
2. Lee, K.; Asher, S.A.; *J. Am. Chem. Soc* 2000, 122, 9534.
3. López, C.; *Adv. Mater* 2003, 15, 1679.
4. Lin, S.Y.; Fleming, J.G.; Hetherington, D.L.; Smith, B.K.; Biswas, R.; Ho, K.M.; Sigalas, M.M.; Zubrzycki, W.; Kurtz, S.R.; Bur, J.; *Nature* 1998, 394, 251.
5. Noda, S.; Tomoda, K.; Yamamoto, N.; Chutinan, A.; *Science* 2000, 289, 604.
6. Yamamoto, N.; Noda, S.; Chutinan, A.; *J. Appl. Phys* 1998, 37, 1052.
7. Fleming, J.G.; Lin, S.Y.; *Opt. Lett* 1999, 24, 49.
8. Zakhidov, A.A.; Baughman, R.H.; Iqba, I.Z.; Cui, C.; Khayrullin, I.; Dantas, S.O.; Marti, J.; Ralchenko, V.G.; *Science* 1998, 282, 901.
9. Blanco, A.; Chomski, E.; Grabtchak, S.; Ibisate, M.; John, S.; Leonard, S.W.; Lopez, C.; Meseguer, F.; Miguez, H.; Mondia, J.P.; Ozin, G.A.; Toader, O.; van Driel, H.M.; *Nature* 2000, 405, 440.
10. Lyon, A.L.; Debord, J.D.; Debord, S.B.; Jones, C.D.; McGrath, J.G.; Serpe, M.J.; *J. Phys. Chem. B* 2004, 108, 19099.
11. Fudouzi, H.; Xia, Y.; *Langmuir* 2003, 19, 9653.
12. Nakamura, H.; Ishii, M.; Tsukigase, A.; Harada, M.; Nakano, H.; *Langmuir* 2006, 22, 1268.
13. Ishii, M.; Nakamura, H.; Nakano, H.; Tsukigase, A.; Harada, M.; *Langmuir* 2005, 21, 5367.
14. Nakamura, H.; Mitsuoka, T.; Ishii, M.; *J. Appl. Polym. Sci* 2006, 102, 2308.
15. Takeoka, Y.; Watanabe, M.; *Langmuir* 2003, 19, 9554.
16. Kumada, M.; Watanabe, M.; Takeoka, Y.; *Langmuir* 2006, 22, 4403.
17. Toyotama, A.; Yamanaka, J.; Shinohara, M.; Onda, S.; Sawada, T.; Yonese, M.; Uchida, F.; *Langmuir* 2009, 25, 589.
18. Foulger, S.H.; Jiang, P.; Pattam, A.C.; Smith, D.W.; Ballato, J.; *Langmuir* 2001, 17, 6023.

19. Takeoka, Y.; Watanabe, M.; Langmuir 2003, 19, 9554.
20. Takeoka, Y.; Watanabe, M.; Adv. Mater 2003, 15, 199.
21. Reese, C.E.; Baltusavich, M.E.; Keim, J.P.; Asher, S.A.; Anal. Chem 2001, 73, 5038.
22. Okubo, T.; J. Am. Chem. Soc 1990, 112, 5420.
23. Iwayama, Y.; Yamanaka, J.; Takiguchi, Y.; Takasaka, M.; Ito, K.; Shinohara, T.; Sawada, T.; Yonese, M.; Langmuir 2003, 19, 977.
24. Asoh, T.; Matsusaki, M.; Kaneko, T.; Akashi, M.; Adv. Mater 2008, 20, 2080.
25. Asher, S.; Holtz, J.; Liu, L.; Wu, Z.; J. Am. Chem. Soc 1994, 116 4997.
26. Iwayama, Y.; Yamanaka, J.; Takiguchi, Y.; Takasaka, M.; Ito, K.; Shinohara, T.; Sawada, T.; Yonese, M.; Langmuir 2003, 19, 977.
27. Gates, B.; Park, S.H.; Xia, Y.; Adv Mater 2000, 9, 653.
28. Yang, H.; Jiang, P.; Langmuir 2010, 26, 13173.
29. Huebner, C.F.; Foulger, S.H.; Langmuir 2010, 26, 2945.
30. Lee, K.; Asher, S.A.; J. Am. Chem. Soc 2000, 122, 9534.
31. Foulger, S.H.; Jiang, P.; Pattam, A.C.; Smith, D.W.; Ballato, J.; Langmuir 2001, 17, 6023.
32. Takeoka, Y.; Watanabe, M.; Langmuir 2002, 18, 5977.
33. Lellig, C.; Hartl, W.; Wagner, J.; Hempelman, R.; Angew. Chem. Int. Ed 2002, 41, 102.
34. Debord, J.D.; Eustis, S.; Debord, S.B.; Lofye, M.T.; Lyon, L.A.; Adv. Mater 2002, 14, 658.
35. Takeoka, Y.; Watanabe, M.; Langmuir 2003, 19, 9554.
36. Yamanaka, J.; Murai, M.; Iwayama, Y.; Yonese, M.; Ito, K.; Sawada, T.; J. Am. Chem. Soc 2004, 126, 7156.
37. Yoshinaga, K.; Shigeta, M.; Komune, S.; Mouri, E.; Nakai, A.; Colloids and Surfaces B: Biointerfaces 2007, 54, 10.
38. Yoshinaga, K.; Chiyoda, M.; Yoneda, A.; Nishida, H.; Komatsu, M.; Colloid. Polym. Sci 1999, 28, 481.

39. Yoshinaga, K.; Chiyoda, M.; Ishiki, H.; Okubo, T.; Colloid. Surf. A 2002, 204, 285.
40. Yoshinaga, K.; Fujiwara, K.; Mouri, E.; Ishii, M.; Nakamura, H.; Langmuir 2005, 21, 4471.
41. Yoshinaga, K.; Mouri, E.; Ogawa, J.; Nakai, A.; Ishii, M.; Nakamura, H.; Colloid. Polym. Sci 2004, 283, 340.
42. Ma, Z.G.; Watanabe, M.; Mouri, E.; Yoshinaga, K.; Colloid. Polym. Sci 2010, 288, 519.
43. Ma, Z.G.; Watanabe, M.; Mouri, E.; Nakai, A.; Yoshinaga, K.; Colloid. Polym. Sci 2011, 289, 85.

Chapter 2

Improvement of refractive index of colloidal crystals by incorporation of ferrocenyl group

2.1 Introduction

Recently, three-dimensional (3D) particle array structure, inter-particle space of which is corresponding to visible light wave length, has been receiving great attention for promising application to optical devices, such as wave guide, sensor and so on [1-8]. So far, there are many approaches for fabrication of the particles array structure [1-35]. One of the approaches is the fabrication of 3D array structure employing colloidal crystal, which is classified by two categories, hard type and soft type. The hard type colloidal crystals are usually formed by deposition or ordering during drying of colloidal suspension, and have an advantage for making large size of single crystal [18-24]. However, the hard type crystal gives blunt Bragg reflection due to direct effects of particle size distribution on particle array structure. On the other hand, soft type colloidal crystals are formed in deionized aqueous solution through electrostatic repulsion between the particles [36, 37]. The soft type crystals usually exhibit a sharp and clear Bragg reflection, challenging of photonic crystal fabrication from the crystals formed in suspension was carried out by solidification of colloidal crystals in hydrogels [13,16,25-31,34,35]. Moreover, the soft type colloidal crystals have the advantage for controlling inter-sphere distance by changing volume fraction of particles, which is fairly attractive for application to photonic devices, in spite of polycrystalline. In cases of soft type systems, colloidal crystallization in aqueous solution has been examined employing monodisperse colloidal silica, polystyrene or poly(methyl methacrylate) latexes, because of easy availability and stability. Especially, colloidal

silica is fairly favorable to make stable colloidal crystallization in aqueous solution due to high surface charge.

In order to fabricate photonic devices composed of 3D arrayed structure, it is obviously essential to immobilize or solidify of colloidal crystals in polymer matrixes. In this respect, we have successfully achieved colloidal crystallization of polymer-grafted silica in organic solvents [38-40], and then immobilization in polymer gels [41-44]. However, there are major problems for fabrication of photonic devices employing colloidal crystals from silica or polymer latexes, because of comparatively low refractive index and/or dielectric constant. On improvement of shortcomings, Ashrit et.al have fabricated photonic crystal of WO_3 by using inverse colloidal crystals of polystyrene latex [8]. So far, incorporation of heavy atoms or high electron density substituent groups into polymer was widely investigated to increase the refractive index [45, 46]. In this study, colloidal crystallization of colloidal silica modified with copolymer of FcMA and MMA group in organic solvent and effects of ferrocenyl group on effective refractive index (n_{eff}) of colloidal crystal system was investigated. Increasing ionic strength in colloidal suspension generally disturbs colloidal crystallization in solution, because of decreasing electric double layer on the surface of particles. Thus, we chose zero valency Fe (0) complex of ferrocenyl group as a functional group for increasing refractive index.

2.2 Experimental

Materials

Colloidal silica, of 150 nm in diameter, suspended in ethanol was kindly offered by JGC Catalysts & Chemicals, Ltd, Japan. 3-Aminopropyltriethoxysilane (3-APTS), N,N'-dicyclohexylcarbodiimide (DCC), N,N,N',N'',N''-pentamethyldiethylene triamine (PMDETA), and N,N'-Azobis(4-cyanovaleric acid) (ACVA) were purchased from Wako Pure Chemical Industries, Ltd., Japan. 2-Bromo-2-methylpropionic acid was purchased from Tokyo Chemical Industry Co. Ltd., Japan.

Measurements

Particle size was determined by a dynamic light scattering (DLS) on DLS-7000DL Otsuka Electronics Co. Ltd, Japan using a He-Ne laser at measurement angle of 90°. Molecular weight of polymer was evaluated by a gel permeation chromatography (GPC) on series-connected columns, PL-gel MIEXED-C and PL-gel MIEXED-D with a differential refract meter and THF eluent of 0.8ml/min. Amounts of grafted polymer was determined by a thermal-gravimetric analysis on TG-50, Shimadzu Co. Ltd., Japan under nitrogen atmosphere during elevating temperature up to 800 at heating rate 10 °C/min. ¹H NMR Spectra were recorded on AVNACE400, Bruker Germany, at 300MHz. Reflection spectra of colloidal crystals was recorded on NAR-2T Atago. Co. Ltd, Transmission electron microscopy (TEM) observation was carried out on H-9000NAR, Hitachi Ltd, Japan.

Preparation of carboxyl-terminated poly(FcMA-co-MMA)

The polymer was synthesized by radical copolymerization of FcMA and MMA in THF (Scheme 1). In Table 1, recipe in radical copolymerization of FcMA and MMA using an initiator of ACVA and molecular weight of resulting copolymers are shown. In this copolymerization, carboxyl-terminated copolymers of FcMA/MMA mole ratio from 1/3 to 1/12 in the molecular weight range from 9600 to 19500 were obtained.

Preparation of triethoxysilyl-terminated poly(FcMA-co-MMA)

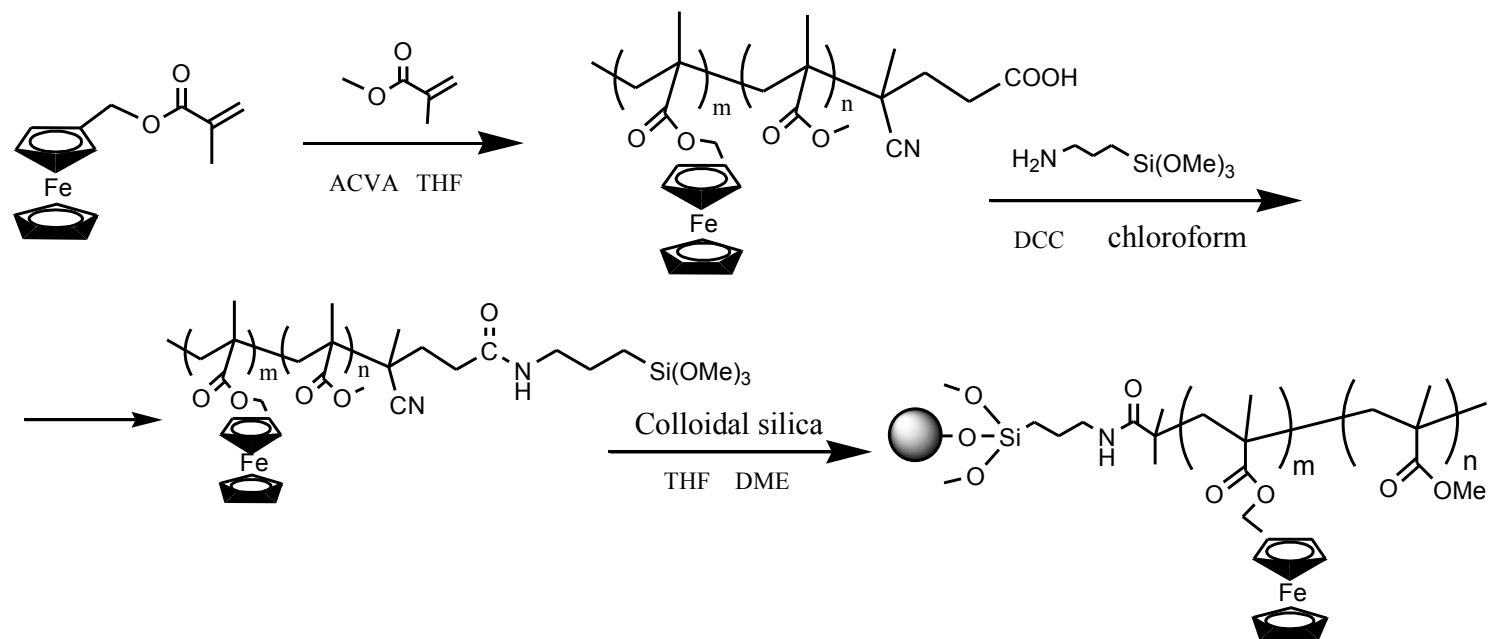
The polymer was synthesized according to previous paper [39]. In a 50 ml flask, 0.622 g carboxyl-terminated poly(FcMA-co-MMA), 2.1 mg DCC and 0.02 ml APTS in 10 ml chloroform was put and the mixture was stirred at 0 °C in N₂ atmosphere for 30 min. Evaporation of solvent and drying under reduced pressure gave 0.47 g copolymer silane.

Grafting of copolymer silane on colloidal silica

In a 100ml flask, 0.12 g copolymer silane and 15ml colloidal silica ethanol suspension, containing 3.0 g SiO₂, and 40 ml 1,2-dimethoxyethane was put, and the mixture was sonicated for 30 min at room temperature. After the suspension was stirred at 90 °C to remove 30 ml of solvent azeotropically, then 10 ml THF was added to the suspension, followed by heating at 70 °C for 12 h. After washing with THF using centrifugation, drying under reduced pressure gave about 2.5 g poly(FcMA-co-MMA)-grafted silica.

Synthesis of 3-(2-bromo-2-methylbutyloyl)aminopropyltriethoxysilane

A mixture of 1.2 g 2-bromo-2-methylpropionic acid, 1.4g DCC and 10 ml chloroform was stirred at 0 °C for 30 min. After addition of 1.4 g APTS to the mixture, the solution was stirred at room temperature for 5 h. Filtration, evaporation of solvent and drying under reduced pressure gave 2.81g product. ¹H NMR (CDCl₃); 0.6 (q, CH₂-Si), 1.2 (q, CH₃), 1.7 (q, CH₂), 2.0 (s, (CH₃)₂), 3.3 (t, CH₂), 7.0 (s, NH) ppm.



Scheme 1. Preparation of poly(FcMA-*co*-MMA)-grafted silica

Table 1. Preparation of carboxyl-terminated poly(FcMA-*co*-MMA)^{a)}

RUN	FcMA / g (mol)	MMA / ml (mol)	ACVA / mg (mol)	M _n (M _w /M _n)	m/n
1	0.23 (8.0×10 ⁻⁴)	0.26 (2.4×10 ⁻³)	1.0 (3.3×10 ⁻⁶)	9,600(1.4)	1/3
2	0.29 (1.0×10 ⁻³)	0.56 (5.3×10 ⁻³)	3.0 (1.0×10 ⁻⁵)	12,000(1.6)	1/5
3	0.45 (1.6×10 ⁻³)	1.35 (1.3×10 ⁻²)	3.0 (1.0×10 ⁻⁵)	16,200(1.7)	1/7
4	0.19 (7.0×10 ⁻⁴)	0.73 (7.0×10 ⁻³)	22.0 (7.0×10 ⁻⁵)	19,500 (2.7)	1/12

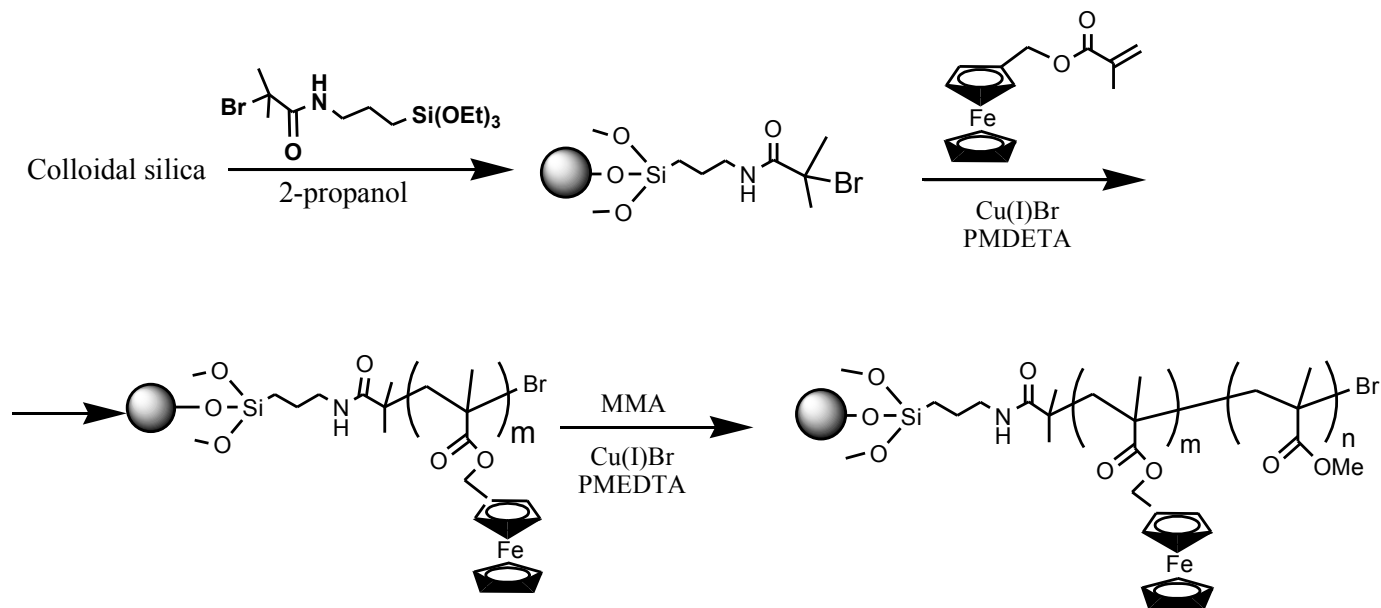
a) In copolymerization 8 ml THF was used.

Preparation of poly(FcMA-block-MMA)-grafted silica

Grafting of block copolymer on colloidal silica was carried out by an atom transfer radical polymerization (Scheme 2). Introduction of initiator group on silica was conducted by the reaction of 3-(2-bromo-2-methylbutyloyl)aminopropyl triethoxysilane with colloidal silica by the same method as described above.

Into a test tube, a mixture of 0.7 g initiator-grafted silica, 0.53 g FcMA, 22 mg CuBr, 32 μ l PMDETA, 3 ml DMF and 0.04ml 1-(2-bromo-2-methylbutyl) aminobutane as a free initiator was put. The test tube was purged with nitrogen through freeze-pump-thaw and heated at 70°C for 24 h. After cooling down, the particles were separated by centrifugation and washed with DMF. Drying under reduced pressure gave 0.7g poly(FcMA)-grafted silica; amount of grafted polymer: 20mg/g, molecular weight of polymer obtained from a free initiator: 2700. A DLS analysis of resulting particles showed achieving polymer grafting without aggregation during the polymerization.

Successive polymerization of MMA on poly(FcMA)-grafted silica was carried out by the same manner as the first one. The mixture of 0.7 g poly(FcMA)-grafted silica, 3.25 ml MMA, 29 mg CuBr, 43 μ l PMDETA, 0.075 ml free initiator, and 3 ml DMF was purged with nitrogen, and then stirred at 70 °C for 2 days to give 0.5 g poly(FcMA-block-MMA)-grafted silica. In this copolymerization, the block-polymer with FcMA/MMA from 1/1.3 to 1/4.9, and molecular weight from 8000 to 40,000 was prepared respectively (in table 2).



Scheme 2. Preparation of poly(FcMA-*block*-MMA)-grafted silica

Table 2. Preparation of poly(FcMA-*block*-MMA)-grafted silica

RUN	PFcMA -grafted silica (Mn=3,000)	MMA	free initiator ($1.1 \times 10^{-3} \text{M}$)	Cu(I)Br	PMDETA	DMF	Mn	m/n
1	0.216 g (1 eq)	2.6 ml (700 eq)	40 μl (11 eq)	13 mg (16 eq)	40 μl (32 eq)	3 ml	8,000(1.6)	1/ 1.3
2	120 mg (1 eq)	3.5 ml (5600 eq)	35 μl (7 eq)	13 mg (16 eq)	40 μl (32 eq)	3 ml	12,000(1.4)	1/2.8
3	110 mg (1 eq)	4.5 ml (8000 eq)	35 μl (7 eq)	13 mg (16 eq)	35 μl (32 eq)	3 ml	18,000(1.8)	1/3.8
4	0.08 g (1 eq)	1.4 ml (6050 eq)	20 μl (10 eq)	7 mg (22 eq)	40 μl (44 eq)	3 ml	40,000(1.6)	1/4.9

Determination of Effective refractive index

Effective refractive index (n_{eff}) of colloidal crystal system was determined from angle-resolved reflection spectra according to Bragg equation on assumption of face centered cubic closed packing [22]:

$$\lambda_{\text{peak}} = 2(2/3)^{0.5} d \sqrt{n_{\text{eff}}^2 - \sin^2 \theta} \quad (1)$$

Where λ_{max} is wave length of reflection peak, θ is incident angle, and d is neighboring particle distance. Actually, n_{eff} was estimated from fitting plots of θ vs. λ_{max} by putting appropriate d value in Eq. (1).

Determination of inter-particle distance

Neighboring inter-particle distance (d_{cal}) was estimated by following equation [37]:

$$d = (3/8)^{0.5} \frac{\lambda}{n_{\text{ave}}} \quad (2)$$

Where λ is peak top wavelength on reflection spectrum recorded at incident angle 90° and n_{ave} is average refraction index of the suspension system calculated by following equation:

$$n_{\text{ave}} = \phi n_{\text{silica}} + (1 - \phi) n_{\text{solvent}} \quad (3)$$

Where, n_{silica} and n_{sol} are refractive index of silica and solvent respectively; and ϕ is volume fraction of silica.

2.3 Results and discussion

2.3.1 Grafting of poly(FcMA-MMA) with the colloidal silica

Grafting of poly(FcMA-co-MMA) on silica was carried out by the reaction of colloidal silica with corresponding polymer silane in 1,2-dimethoxyethane under refluxing. Amounts of grafted polymer were in the range from 14 mg/g to 36 mg/g (Table 3). And the poly(FcMA-block-MMA) show amount of grafted polymer with 91 mg/g to 344mg/g. These particles were well dispersed in organic solvents, such as THF acetonitrile.

2.3.2 Colloidal crystallization

When poly(FcMA-MMA)-grafted silica was dispersed in DMF and acetonitrile, colloidal crystallization was observed. In Table 3, critical volume fraction for colloidal crystallization of poly(FcMA-co-MMA)- and PMMA-grafted silica was shown. The critical volume fraction (ϕ_0) is the minimal fraction of colloidal particles to form colloidal crystals. Therefore, low ϕ_0 values is attributable to strong electrostatic interaction, and then ϕ_0 values is sometimes employed as an index of stability of colloidal crystals. The values of ϕ_0 for copolymer-grafted silica in DMF were in the range from 0.081 to 0.094, higher than those, 0.029 to 0.048 in acetonitrile. Probably, high polarity of DFM disturbs the crystallization due to decreasing electrostatic repulsion between the particles. Also, ϕ_0 values for copolymer-grafted silica in DMF and acetonitrile were fairly higher than those for PMMA-grafted silica. The reason for low ϕ_0 values in colloidal crystallization of the present copolymer-grafted silica is still unclear. It might come from increasing π - π interaction between ferrocenyl groups in grafted polymer chains to disturb electrostatic repulsion between the particles. And the higher volume fraction of the polymer grafted silica or higher mole fraction of ferrocenyl group would be beneficial to the refractive index of the colloidal crystal systems, so there the colloidal crystals formed in DMF is as emphasis.

As seen in table 4, the values of ϕ_0 for block-polymer-grafted silica in DMF is

lower than that of copolymer-grafted silica, range from 0.054 to 0.083. Also, ϕ_0 values for copolymer-grafted silica in DMF and acetonitrile were fairly higher than those for PMMA-grafted silica. It might come from increasing π - π interaction between ferrocenyl groups in grafted polymer chains to disturb electrostatic repulsion between the particles. In this case, the crystallization probably takes place based on steric repulsion between grafted polymer chains on silica particles [47]. Therefore, relatively low ϕ_0 values presumably come from the localization of the ferrocenyl group in block-polymer grafted silica.

In Figure 1, typical pictures of colloidal crystals are shown. Interestingly, in the front side view against light irradiation colloidal crystallites was observed in green solution, and transmission light in the rear side was colored reddish. The coloration in colloidal crystallization of polymer-grafted silica containing diene-iron (0) tricarbonyl complex in organic solvent was observed previously, coming from cooperative effects of specific absorption of 400-500 nm light by iron (0) complex moiety and transmission of 700-800 nm light through the crystals [48].

Table 3. Critical volume fraction (ϕ_o) of poly(FcMA-co-MMA)/SiO₂ in organic solvent

Grafted polymer			A.P /mg/g-SiO ₂	ϕ_o	
	m/n	M _n (M _w /M _n)		DMF	acetonitrile
Poly(FcMA-co-MMA)/SiO ₂	1/3	9,600(2.6)	16	0.094	0.039
	1/5	12,000(1.6)	36	0.089	0.048
	1/7	16,200(1.9)	17	0.081	0.041
	1/12	19,500(2.7)	14	0.083	0.029
	0/1	25,000(1.7)	21	0.059	0.017

Table 4. Critical volume fraction (ϕ_0) of poly(FcMA-block-MMA)/SiO₂ in organic solvent

Grafted polymer			A.P /mg/g-SiO ₂	ϕ_0
Poly(FcMA-block-MMA) /SiO ₂	m/n	M _n		DMF
	1/1.3	8,000	91	0.083
	1/2.8	12,000	124	0.069
	1/3.8	18,000	344	0.059
	1/4.9	40,000	223	0.054
	PMMA/SiO ₂	0/1	25,000	21

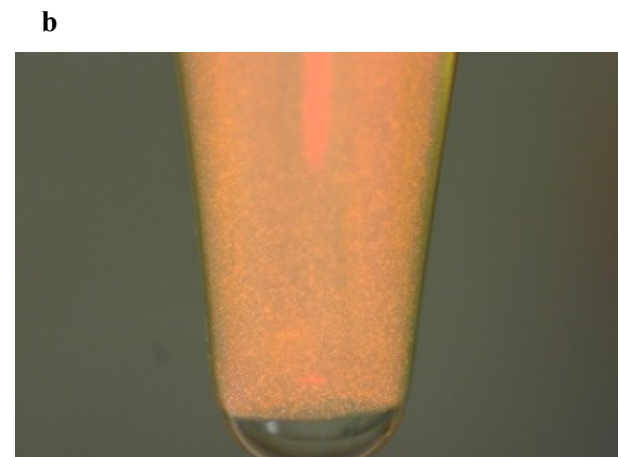
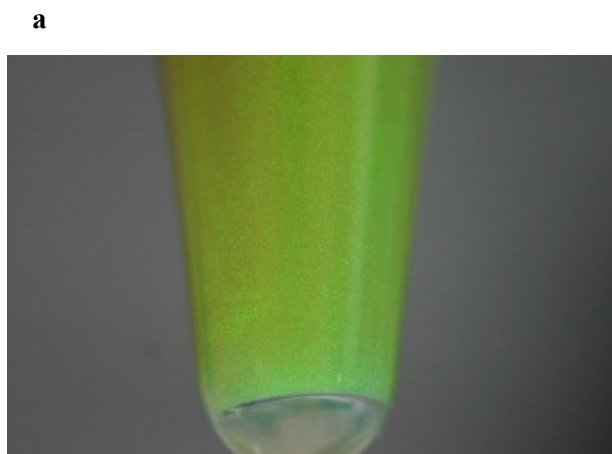


Figure 1. Photographs of colloidal crystals of poly(FcMA-co-MMA) ($m/n=1/3$)-grafted silica in DMF. Front side (a) and rear side (b) against light irradiation.

2.3.3 Effective refractive index

In Figure 2, angle resolved reflection spectra of colloidal crystals of poly(FcMA-co-MMA)-grafted SiO₂ in DMF at incident angle from 20 to 44 degree were shown. Typical fitting plotting between θ and λ_{\max} in Eq (1) for optimizing inter-particle distance (d) and effective diffraction (n_{eff}) was shown in Figure 2. And n_{eff} and d values can estimated by fitting plots for colloidal crystals systems of P(FcMA-MMA)-grafted silica in DMF. Also, the average refractive index (n_{ave}) and inter-particle distances (d_{colloid}) is derived by Eq.(2) and (3), respectively. Consequently, the value of n_{ave} is simply estimated from ones of silica and solvent without taking account grafted polymer. And d values were well coincident with d_{colloid} within 5% deviation. Therefore, it was suggested that n_{eff} values were reasonable and relatively precise. In table 5, the values of n_{eff} slightly increased with increasing mole fraction of FcMA in grafted polymer. However, these values changed with volume fraction of polymer-grafted silica and mole fraction of FcMA in the copolymer. Thus, differential effective refractive indexes ($\Delta n/\phi$), which were normalized by average refractive index (n_{ave}) and volume fraction of particles (ϕ) were proposed: $\Delta n = n_{\text{eff}} - n_{\text{ave}}$. The value of Δn is the difference between the colloidal crystal and the silica composite solution of organic solvent. Here, it is important to notify that n_{eff} implies contribution of grafted copolymer involved with Fe(0) complex in ferrocenyl group to refractive index of colloidal crystal system.

In Figure 3, plots of mole fraction of FcMA in grafted polymer vs $\Delta n/\phi$ were shown. The normalized values of colloidal crystal proportionally increased with mole fraction of FcMA. And the value of the $\Delta n/\phi$ of block-polymer grafted silica is higher than that of the co-polymer grafted silica. In block-polymer grafted silica, the normalized values reached 0.83, which was about 5 times of that of PMMA-grafted silica. And in co-polymer grafted silica, the normalized values also reached 0.27, which was 50% higher as compared with that of PMMA-grafted silica. The difference of the normalized values between the co-polymer grafted silica and block-polymer grafted silica maybe come from the clustering degree of the ferrocenyl group. In co-polymer grafted silica, the particles were modified with random copolymer of FcMA and MMA, and ferrocenyl groups in grafted copolymer were considered to exist in relatively

homogeneous around particle surface. And in block-polymer grafted silica, the ferrocenyl groups in grafted copolymer localized on the surface of particle. The condensation of ferrocenyl groups near surface of the particles, could efficiently contribute to increasing refractive indexes. Those results showed that introduction of ferrocenyl group in polymer grafted silica effectively enhanced refractive index of colloidal crystal systems.

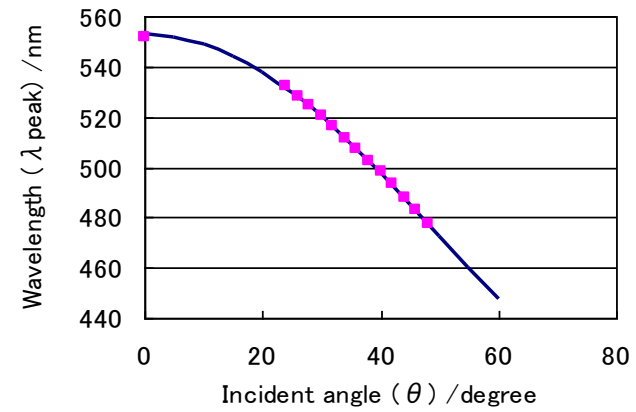
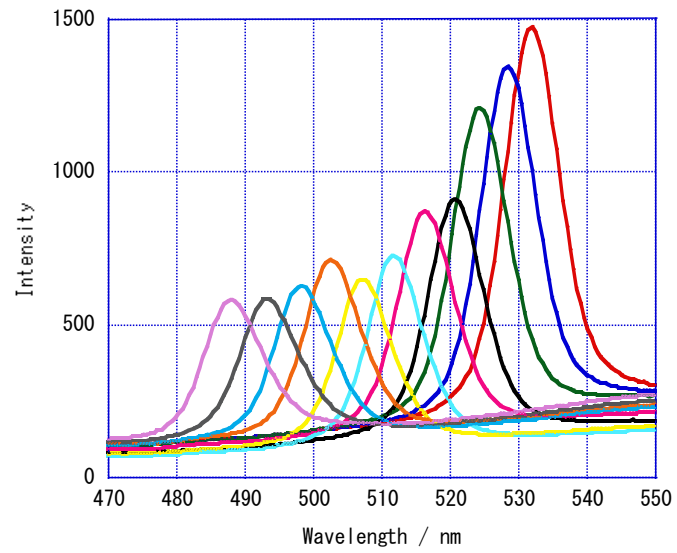


Figure 2. Angle resolved reflection spectra of colloidal crystals of poly(MMA-*co*-FcMA) ($m/n=1/5$)-grafted silica in DMF (a), and fitting curve between θ and λ_{peak} in Eq (1) (b).

Table 5. Effective refractive index (n_{eff}) and $\Delta n / \phi$ of colloidal crystals in DMF

particles	m/n in Graft polymer	ϕ	n_{eff}	$n_{\text{ave}}^{\text{b)}$	$\Delta n^{\text{a)}$	$\Delta n / \phi$
Poly(FcMA-co-MMA)/SiO ₂	1/3	0.188	1.489	1.437	0.052	0.276
	1/5	0.177	1.481	1.436	0.045	0.254
	1/7	0.166	1.476	1.435	0.041	0.247
Poly(FcMA-block-MMA)/SiO ₂	1/1.3	0.094	1.510	1.432	0.078	0.830
	1/2.8	0.111	1.493	1.436	0.057	0.514
	1/3.8	0.169	1.518	1.436	0.082	0.485
	1/4.9	0.176	1.513	1.436	0.077	0.435
PMMA/SiO ₂	0/1	0.225	1.478	1.439	0.039	0.173

a) $\Delta n = n_{\text{eff}} - n_{\text{ave}}$

b) Average refractive index (n_{ave}): $n_{\text{ave}} = \phi n_{\text{silica}} + (1-\phi)n_{\text{solvent}}$

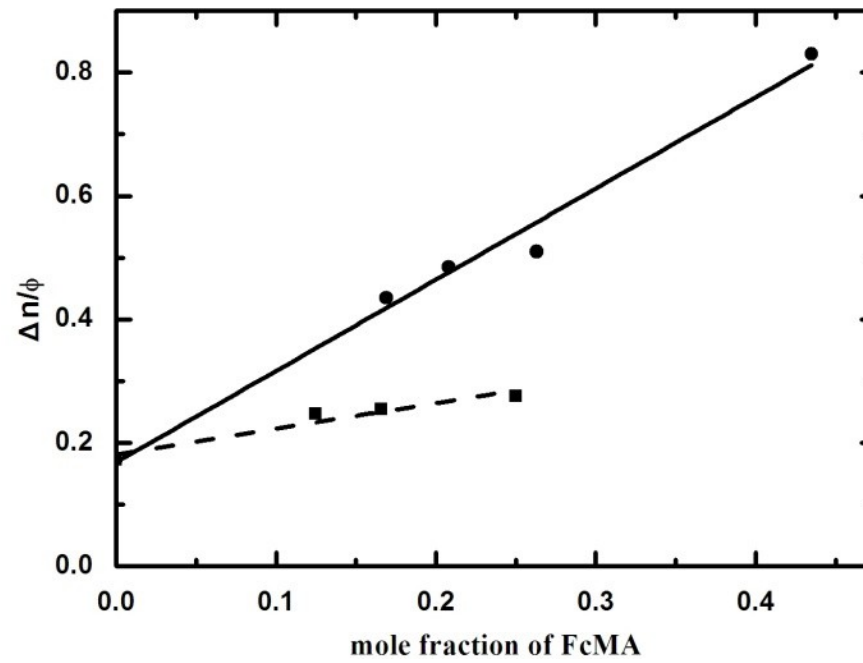


Figure 3. Plots of FcMA mole fraction in grafted polymer (— block-polymer --- co-polymer) vs. normalized effective refractive index ($\Delta n/\phi$)

2.3.4 TEM observation of copolymer-grafted silica

Figure 4 shows the TEM images of PMMA-, poly(FcMA-co-MMA)- and poly(FcMA-block-MMA)-grafted silica. It was observed that the surface of poly(FcMA-co-MMA)-grafted silica was smooth and homogeneous, as well as that of PMMA-grafted silica, while the surface of block-polymer grafted silica was heterogeneous and spotty area. The area was possibly assigned to clustering of ferrocenyl methacrylate moiety, formed due to π - π or nonpolar-nonpolar interaction between ferrocenyl groups. Therefore, high effectiveness of ferrocenyl group in refractive index of block-polymer-grafted silica system probably stemmed from bias existence of ferrocenyl groups in block-polymer grafted silica.

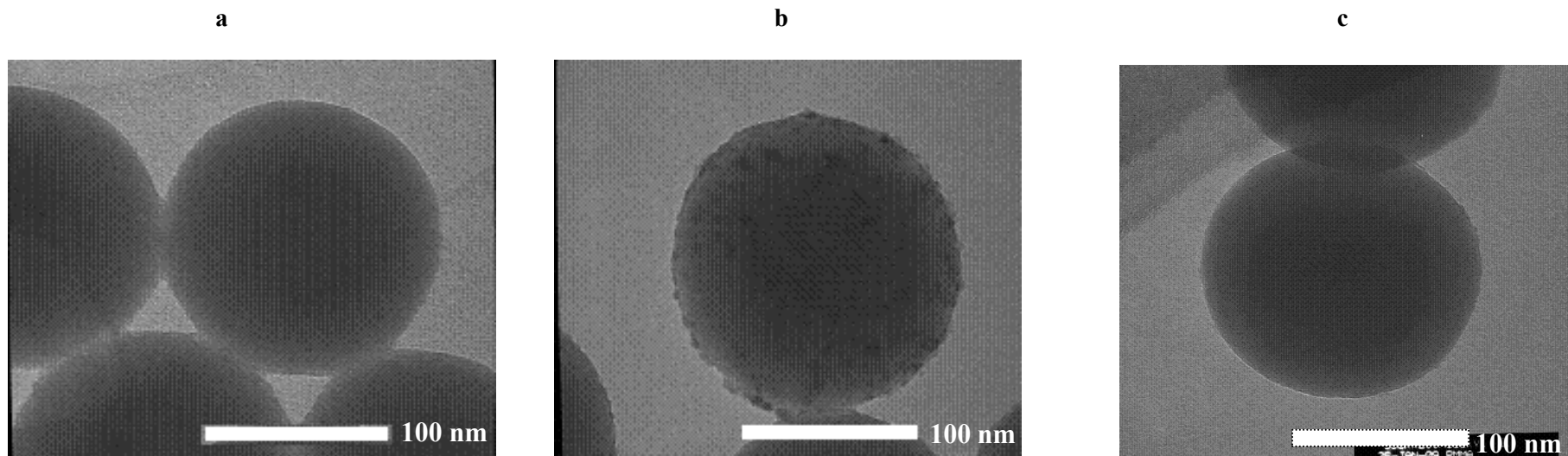


Figure 4. TEM images of poly(FcMA-co-MMA)(m/n=1/3)- (a), poly(FcMA- block-MMA) (m/n=1/5)- (b) and PMMA-grafted silica (c)

2.4 Conclusions

Colloidal silica modified with copolymer tethering ferrocenyl group, poly(FcMA-co-MMA) and poly(FcMA-block-MMA), brought colloidal crystallization in DMF and acetonitrile. Characteristic coloration of colloidal crystals was observed due to cooperative effects of specific absorption at 400-500 nm by ferrocenyl group and transmission of 700-800 nm light through the crystals. Normalized effective refractive index by volume fraction of the particles increased with mole fraction of FcMA in copolymer. This result suggested that introduction of ferrocenyl group into grafted copolymer led to enlargement of refractive index of colloidal silica systems.

2.5 References

1. Holtz, J.H.; Asher, S.A.; *Nature* 1997, 389, 829.
2. Reese, C.E.; Mikhonin, A.V.; Kamenjicki, M.; Tikhonov, A.; Asher, S.A.; *J. Am. Chem. Soc* 2004, 126, 1493.
3. Muscatello, M.M.W.; Stunja, L.E.; Asher, S.A.; *Anal. Chem* 2009, 81, 4978.
4. Muscatello, M.M.W.; Stunja, L.E.; Thareja, P.; Wang, L.; Bohn, J.J.; Velankar, S.S.; Asher, S.A.; *Macromolecules* 2009, 21, 4403.
5. Xia, Y.; Gates, B.; Yin, Y.; Lu, Y.; *Adv. Mater* 2000, 12, 693.
6. Lawrence, J.R.; Ying, Y.; Yiang, P.; Foulger, S.H.; *Adv. Mater* 2006, 18, 300.
7. Park, J.H.; Ohoi, W.S.; Koo, H.Y.; Kim, D.Y.; *Adv. Mater* 2005, 17, 879.
8. Kuai, S.L.; Bader, G.; Ashrit, P.V.; *Appl. Phys. Lett* 2005, 86, 22110.
9. Cong, H.; Cao, W.; *Langmuir* 2004, 20, 8049.
10. Nagao, D.; Anzai, N.; Kobayashi, Y.; Gu, S.; Konno, M.; *J. Colloid. Interface. Sci* 2006, 298, 232.
11. Hong, S.H.; Moon, J.H.; Lim, J.M.; Kim, S.H.; Yang, S.M.; *Langmuir* 2005, 21, 10416.
12. Zheng, N.; Fan, J.; Stucky, G.D.; *J. Am. Chem. Soc* 2006, 128, 6550.
13. Zhou, J.; Cai, T.; Tang, S.; Marquez, M.; Hu, Z.; *Langmuir* 2006, 22, 863.
14. Li, Y.; Kunitake, T.; Fujikawa, S.; Ozasa, K.; *Langmuir* 2007, 23, 9101.
15. Zhou, Z.; Yan, Q.; Li, Q.; Zhao, X.S.; *Langmuir* 2007, 23, 1473.
16. Hosein, I.D.; Lindell, C.M.; *Langmuir* 2007, 23, 2892.
17. Weekes, S.M.; Ogrin, F.Y.; Murray, W.A.; Keatley, P.S.; *Langmuir* 2007, 23, 1057.
18. Jiang, P.; Bertone, J.F.; Hwang, K.S.; Colvin, V.L.; *Chem. Mater* 1999, 11, 2132.
19. Lyon, A.L.; Debord, J.D.; Debord, S.B.; Jones, C.D.; McGrath, J.G.; Serpe, M.J.; *J. Phys. Chem. B* 2004, 108, 19099.
20. Fudouzi, H.; Xia, Y.; *Langmuir* 2003, 19, 9653.
21. Camargo, P.H.; Lee, Y.H.; Jeong, U.; Zou, Z.; Xia, Y.; *Langmuir* 2007, 23, 2985.
22. Nakamura, H.; Ishii, M.; Tsukigase, A.; Harada, M.; Nakano, H.; *Langmuir* 2006,

- 22, 1268.
23. Ishii, M.; Nakamura, H.; Nakano, H.; Tsukigase, A.; Harada, M.; Langmuir 2005, 21, 5367.
24. Nakamura, H.; Shii, M.; Tsukigase, A.; Harada, M.; Nakano, H.; Langmuir 2005, 21, 8918.
25. Nakamura, H.; Ishii, M.; Langmuir 2005, 21, 11578.
26. Nakamura, H.; Mitsuoka, T.; Ishii, M.; J. Appl. Polym. Sci 2006, 102, 2308.
27. Takeoka, Y.; Watanabe, M.; Langmuir 2003, 19, 9554.
28. Kumada, M.; Watanabe, M.; Takeoka, Y.; Langmuir 2006, 22, 4403.
29. Sakai, T.; Takeoka, Y.; Seki, T.; Yoshida, R.; Langmuir 2007, 23, 8651.
30. Sawada, T.; Suzuki, Y.; Toyotama, A.; Iyi, N.; Jpn. J. Appl. Phys 2001, 40, 1226.
31. Yamanaka, J.; Murai, M.; Iwayama, Y.; Yonese, M.; Ito, K.; Sawada, T.; J. Am. Chem. Soc 2004, 126, 7156.
32. Murai, M.; Yamada, H.; Yamanaka, J.; Onda, S.; Yonese, M.; Ito, K.; Sawada, T.; Uchida, F.; Ohki, Y.; Langmuir 2007, 23, 7510.
33. Toyotama, A.; Kanai, T.; Sawada, T.; Yamanaka, J.; Ito, K.; Kitamura, K.; Langmuir 2005, 21, 10268.
34. Toyotama, A.; Yamanaka, J.; Shinohara, M.; Onda, S.; Sawada, T.; Yonese, M.; Uchida, F.; Langmuir 2009, 25, 589.
35. Evanoff, D.D.; Hayes, S.E.; Ying, Y.; Shim, G.H.; Lawrence, J.R.; Carroll, J.B.; Roeder, R.D.; Houchins, J.M.; Huebner, C.F.; Foulger, S.H.; Adv. Mater 2009, 19, 3507.
36. Okubo, T.; Acc. Chem 1986, 82, 3163.
37. Okubo, T.; Colloid. Surf. A 1996, 109, 97.
38. Yoshinaga, K.; Chiyoda, M.; Yoneda, A.; Nishida, H.; Komatsu, M.; Colloid. Polym. Sci 1999, 28, 481.
39. Yoshinaga, K.; Chiyoda, M.; Ishiki, H.; Okubo, T.; Colloid. Surf. A 2002, 204, 285.
40. Yoshinaga, K.; Shigeta, M.; Komune, S.; Mouri, E.; Nakai, A.; Colloids. Surf. B 2007, 54, 10.

41. Yoshinaga, K.; Fujiwara, K.; Tanaka, Y.; Nakanishi, M.; Takesue, M.; ChemLett 2003, 32, 1082.
42. Yoshinaga, K.; Mouri, E.; Ogawa, J.; Nakai, A.; Ishii, M.; Nakamura, H.; Colloid. Polym. Sci 2004, 283, 340.
43. Yoshinaga, K.; Fujiwara, K.; Mouri, E.; Ishii, M.; Nakamura, H.; Langmuir 2005, 21, 4471.
44. Yoshinaga, K.; Satoh, S.; Mouri, E.; Nakai, A.; Colloid. Polym. Sci 2006, 284, 694.
45. Arsenault, A.; Miguez, H.; Kitaev, V.; Ozin, G.A.; Manners, I.; Chem. Mater 2003, 15, 503.
46. Paquet, C.; Cyr, P.W.; Kumacheva, E.; Manners, I.; Chem. Mater 2004, 16, 5250.
47. Ohno, K.; Morinaga, T.; Takeno, S.; Tsujii, Y.; Fukuda, T.; Macromolecules 2006, 39, 1245.
48. Yoshinaga, K.; Mouri, E.; Proceedings SPIE 2007, 6767, 8.

Chapter 3

The disordering of particle-arrayed structure of colloidal crystals during immobilization

3.1 Introduction

Application of colloidal crystals to optical devices such as wave guide, sensor, and so on [1-9], has been recently attracting much interest because inter-sphere distance in the crystal structure, i.e. three-dimensional (3D) particle array, is comparable to visible light wavelength. So far, there are many approaches for fabrication of the 3D structure starting from colloidal crystals, which are classified by two categories, hard type and soft type [10-25]. The hard-type colloidal crystals, contacting between neighboring particles, are usually formed by sedimentation or ordering during drying of colloidal suspension, and have advantage for making large size of single crystal [10-16]. However, the hard-type crystals are principally unfavorable for controlling inter-sphere distance to tune photo-diffraction. On the other hand, the soft-type crystals are originally formed in deionized aqueous solution through electrostatic repulsion between particles [26, 27]. The soft-type crystal usually exhibits sharp Bragg diffraction and has an advantage of ease changing inter-sphere distance with particle volume fraction, which is fairly attractive for application to photonic devices despite of polycrystalines. In many cases, especially, colloidal crystallization in aqueous solution has been examined employing monodisperse colloidal silica, because of easy availability and stability due to high surface charge.

In order to fabricate photonic devices from colloidal crystals, it is substantially required to be immobilized 3D particle array structure in colloidal crystals. In cases of 3D particle array composite fabrication employing soft-type colloidal crystals,

many approaches were examined by use of hydrogel-immobilized colloidal crystals [17-25]. The hydrogels, however, are sometimes inconvenient for practical application to phonic devices, because of containing much amounts of water. In this respect, we have successfully achieved colloidal crystallization of polymer-grafted silica in organic solvents [28-30] and then immobilization by two-step radical polymerization by UV irradiation in polymer gels [31-33]. In general, however, radical polymerization of vinyl monomer is usually accompanied by contraction in volume. Thus, it is markedly important to optimize the polymerization condition to prevent from distortion or disordering of 3D particle array structure during immobilization. In this study, effects of particle volume fraction on strain of particle array in colloidal crystals of poly(methyl methacrylate)(PMMA)-grafted silica in immobilization process through two-step radical polymerization were investigated.

3.2 Experiments

Materials

Colloidal silica, of 150 nm in diameter, suspended in ethanol was kindly offered by JGC Catalysts & Chemicals, Ltd, Japan. Methyl methacrylate(MMA), ethylene dimethacrylate (EDTA), 1-hydroxycyclohexylphenylketone, tetrahydrofuran (THF), 2,2'-azobis(isobutyronitrile) (AIBN),3-mercaptopropyltriethoxysilane (3-MPTS) were purchased from Wako Pure Chemical Ind, Japan.

Measurements

Particle size was determined by a dynamic light scattering (DLS) on DLS-7000DLOtsuka Electronics Co. Ltd., Japan, using a He-Ne laser at measurement angle of 90°. Number average molecular weight of polymer was evaluated by a gel permeation chromatography (GPC) on two columns connected in series, PL-gel MIEXED-C and PL-gel MIEXED-D, TOSOH, Co. Ltd., Japan with a differential refract meter using THF eluent of 0.8ml/min. Amounts of grafted polymer was determined by a thermal-gravimetric analysis on TG-50, Shimadzu Co. Ltd., Japan, under nitrogen atmosphere during elevating temperature up to 800°C at heating rate 10 °C/min. ¹H NMR Spectra were recorded on AVNACE400, Bruker, Germany, at 400MHz. Reflection spectra of colloidal crystals was recorded on a multichannel spectrometer, Hamamatsu Photonics PMA-11, Japan. Scanning electron microscope (SEM) images of cross section of colloidal crystals-immobilized PMMA matrix were recorded on a JEOL JSM-5510LV, Japan, after etching on a focused ion beam processing (FIB) Hitachi FB-2000A, Japan. Laser confocal microscope (LCM) observation was carried out on TE2000E Nikon.Co. Ltd, Japan.

Preparation of trimethoxysilyl-terminated poly(methyl methacrylate) (PMMA-Si(OMe)₃)

Into a 50ml flask, 10 ml MMA, 50 mg AIBN, 0.3 ml 3-MPTS, and 10 ml THF were put, and then after purging with nitrogen the mixture was stirred at 70°C for 24h[34]. Resulting polymer, PMMA-Si(OMe)₃, was precipitated with diethylether. After washing with THF by centrifugation, drying under reduced pressure gave 7.83 g PMMA-Si(OMe)₃ of molecular weight 7400.

Preparation of PMMA-grafted silica

Into a 100ml flask, a mixture of 1.5 g PMMA-Si(OMe)₃ and 20 ml colloidal silica dispersed in ethanol, containing 4.0 g SiO₂, and 40ml 1,2-dimethoxyethane was put and sonicated for 30min at room temperature. The mixture was stirred at 90°C for 12h[34]. After azeotropic removing of solvent and 15ml THF was added to the suspension and the solution was stirred at 70 °C for 12h. Centrifugal washing with THF and drying under reduced pressure gave 1.41 g PMMA-grafted SiO₂; amount of grafted polymer on the silica particles was 22mg/g.

The colloidal crystallization and immobilization

A typical run was as follows. A mixture of 0.2g PMMA-grafted silica dispersed in 0.54ml acetonitrile, 30mg EDMA and 6.5 mg 1-hydroxy-cyclohexylphenylketone was put into a vial and sonicated for 30 min at room temperature. In this case, volume fraction (ϕ) of polymer-grafted silica in suspension was 0.18. Particle volume fraction ϕ , was adjusted in the range from 0.07 to 0.25 by changing volume of acetonitrile. Colloidal crystals suspension was put into a 10 mm x 10 mm glass cell in 2 mm thickness, and then the cell was irradiated for 8 h by a high pressure Hg lamp (500 W) in a water bath at room temperature to make PMMA gel. The resulting gel was immersed into MMA containing 1-hydroxycyclohexylphenylketone to exchange acetonitrile in gel with the monomer for 3 days, and then the gel was put into the cell again, followed by UV irradiation for 5 h to solidify the gel.

Determination of inter-sphere distance

Inter-sphere distance (d_{cal}) in colloidal crystal was calculated from the volume fraction on assumption of face centered cubic closed packing by Eq. (1) [35],

$$d_{cal}=0.9047 \times r \times \phi^{-1/3} \quad (1)$$

Where ϕ is volume fraction of PMMA-grafted silica, d_{calcd} is neighboring inter-sphere distance and r is diameter of the particle. The Inter-sphere distance (d_{obs}) in the crystals was also determined according to Bragg formula by following equation [27]:

$$d_{obs} = \sqrt{\frac{3}{8}} \frac{\lambda_p}{n} \quad (2)$$

Where λ_p is the peak top wavelength on a reflection spectrum, n is average refractive index of the suspension system calculated by Eq. (3)

$$n = \phi n_{silica} + (1-\phi)n_{sol} \quad (3)$$

Where, n_{silica} and n_{sol} are refractive index of silica and solvent, respectively, and ϕ is volume fraction of silica. The inter-sphere distance (d_{SEM}) and its standard deviation in PMMA matrix were also determined on SEM images of species after etching on a focused ion beam processing.

Determination of single crystal size

Size of a single crystal (L) in colloidal crystals suspension or in gel was estimated by Scherrer's formula [35, 36],

$$L = \frac{1}{S_s - S_l} \quad (4)$$

where $S_x = 2\sin\theta/\lambda_x$, and λ_1 is the larger wavelength at half-maximum, λ_s is the smaller wavelength at half-maximum, and θ is incident angle. The size was also determined by LCM observation.

3.3 Result and discussion

3.3.1 Colloidal crystallization of PMMA-grafted silica

As reported previously [30], PMMA-grafted silica afforded colloidal crystallization in organic solvent, which were polar and good solvents for grafted polymer. In the present case, colloidal crystallization of PMMA-grafted SiO₂ took place over the critical volume fraction (ϕ_0) of 0.07 in acetonitrile. In this regard, ϕ_0 values usually increased with addition of polymers or monomers colloidal crystals suspension [33]. Therefore, colloidal crystallization of PMMA-grafted SiO₂ and immobilization were investigated in the range of ϕ from 0.07 to 0.25. Actually, when PMMA-grafted SiO₂ was dispersed in acetonitrile solution containing MMA, EDMA and 1-hydroxycyclohexylphenylketone, colloidal crystallization took place in the range from 0.11 to 0.18.

In Figure 1, typical photographs of colloidal crystals in acetonitrile are shown. Bluish reflection color due to Bragg diffraction at a reflection side of a cell and complimentary reddish color at transmission side were observed, respectively. In Figure 2, reflection spectra of colloidal crystals formed in acetonitrile at $\phi=0.11$, 0.14 and 0.18 are shown. Distinct reflection peaks due to Bragg diffraction was observed at 575, 545 and 502 nm, respectively. In LCM images, formation of colloidal crystals of 40-50, 10-20 and 5-10 μm in size at $\phi=0.11$, 0.14 and 0.18, respectively, was also observed (Figure 3).

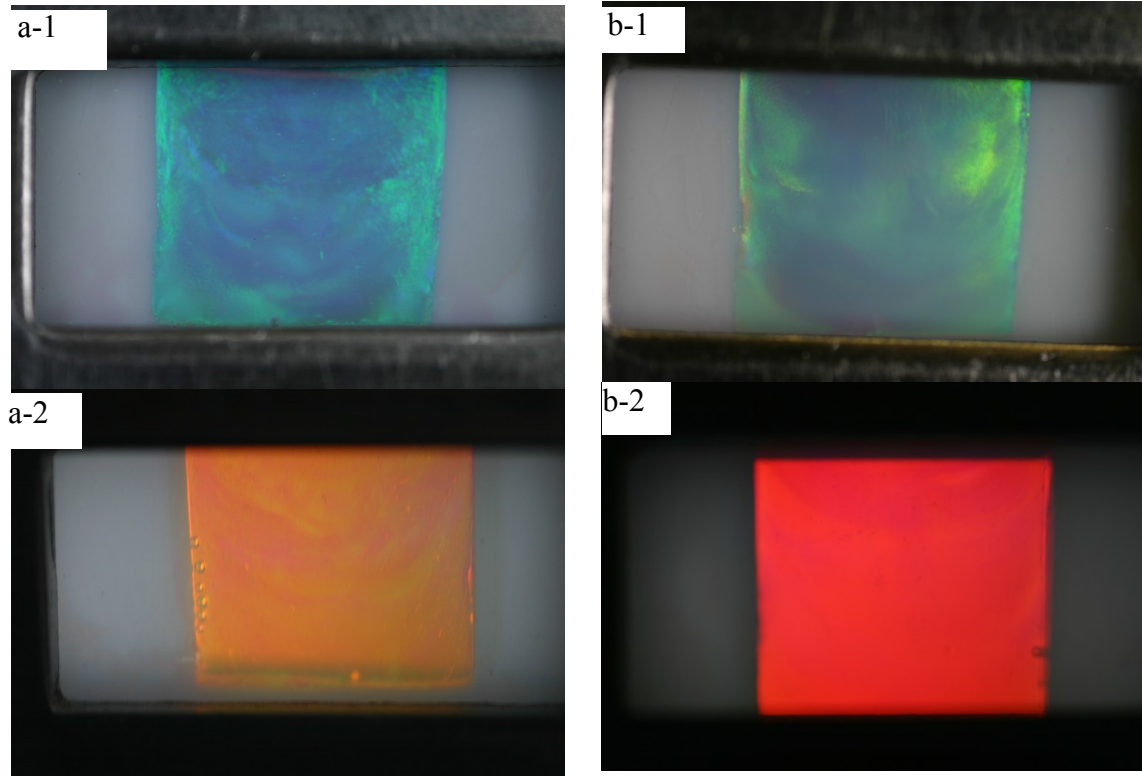


Figure 1. Photographs of colloidal crystals in acetonitrile at $\phi=0.11$ (a) and $\phi=0.14$ (b); a-1 and b-1 at reflection side, a-2 and b-2 at transmission side.

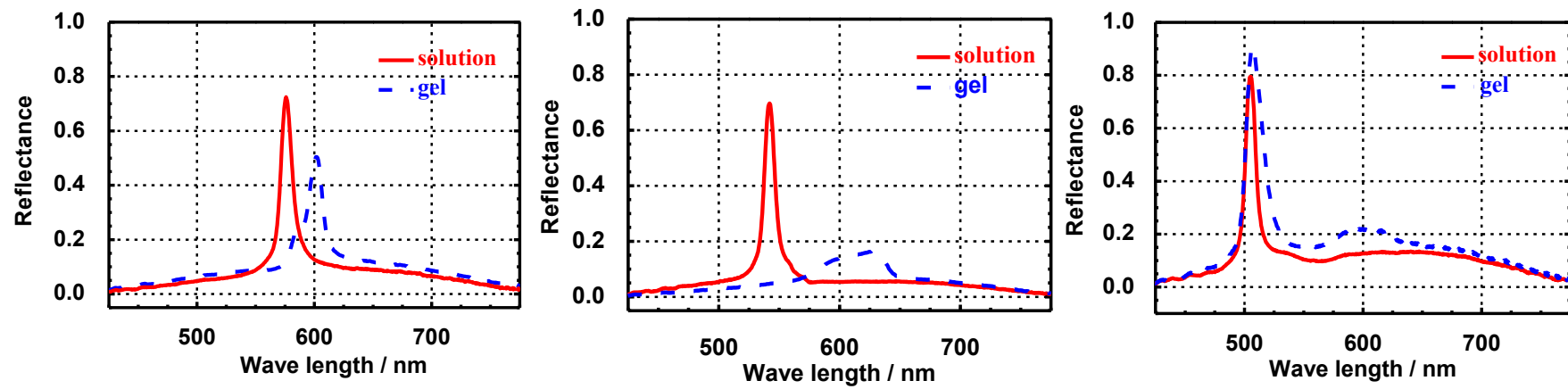


Figure 2. Reflection spectra of colloidal crystals in acetonitrile and in gel; a, b, and c are at $\phi=0.11$, $=0.14$ and 0.18 , respectively.

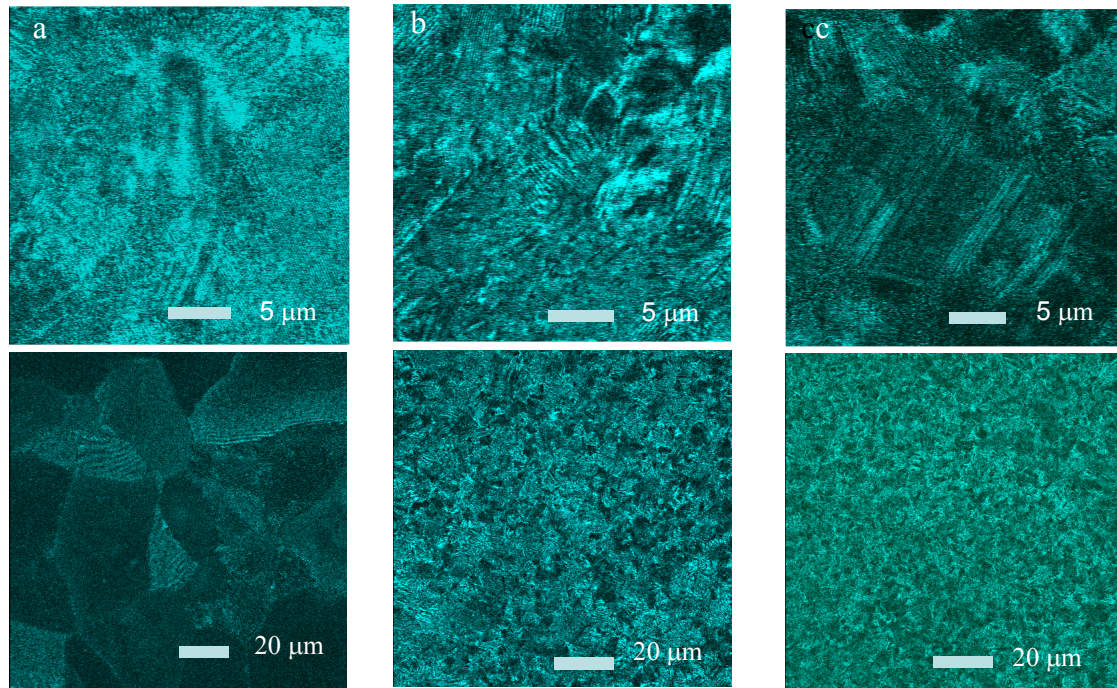


Figure 3. LCM images of colloidal crystals in acetonitrile; a, b, and c are at $\phi=0.11$, 0.14, and 0.18, respectively.

3.3.2 Immobilization of colloidal crystals

Immobilization of colloidal crystals formed in acetonitrile was carried out by two step radical polymerization for gelation, followed by solidification after exchanging of acetonitrile in gel with MMA. In Figure 2, reflection spectra of gels immobilized colloidal crystals are also shown. In these spectra, reflection peaks of gels, 601, 641, and 506 nm at $\phi=0.11$, 0.14, and 0.18 respectively, were observed respective red-shifting of 26, 96, and 4 nm at $\phi=0.11$, 0.14, and 0.18 from corresponding those of colloidal crystals formed in acetonitrile, coming from expanding of inter-sphere distance during polymerization. In these cases, the spectra were of a front side of a cell against UV irradiation. Therefore, these results indicate that inter-particle distances at the front part in a cell become longer, while those at the rear become shorter. The changes of inter-sphere distances through the polymerization probably come from preferential and fast polymerization at a front part against UV irradiation [33]. However, it was observed that reflection peak shifts of gel from those of colloidal crystals in solution often depended on the extent of swelling of gel during polymerization. Intensity of reflection peaks of gels after gelation became weak much more than those of the crystals in acetonitrile, probably due to decrease of crystal numbers. Preservation of particle-arrayed structure in gel was observed by LCM observation of gel cross-section, as shown in Figure 4. However, unfortunately, clear single crystal was not observed by LCM observation of PMMA matrix containing colloidal crystals. The changes of inter-sphere distance in colloid crystals with immobilization process are discussed later.

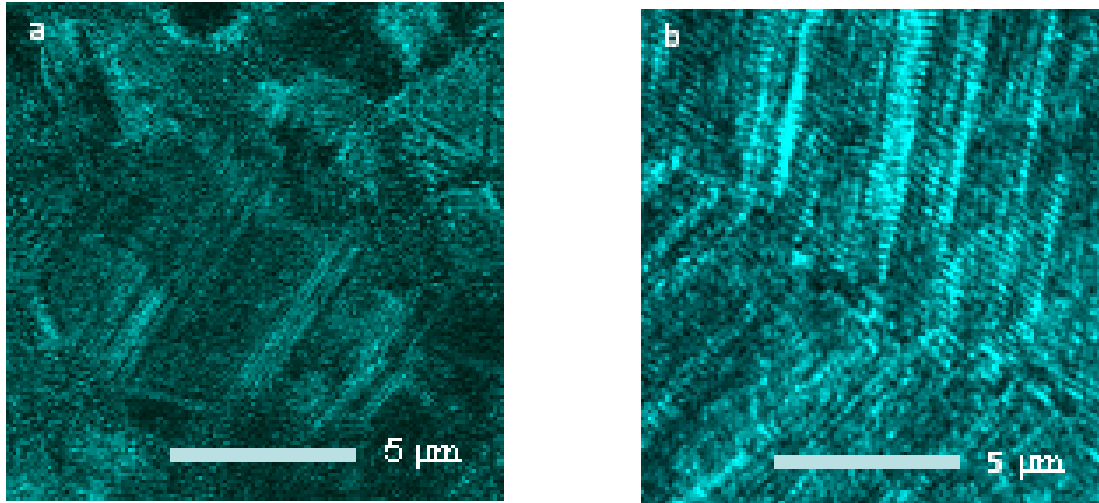


Figure 4. LCM images of colloidal crystals in acetonirile (a) and of cross-section of immobilized gel.

3.3.3 Single crystal size

Single crystal sizes in colloidal crystals in acetonitrile and gel, were listed in Table 1. The size of colloidal crystals in acetonitrile decreased with increasing ϕ from 18.8 μm to 5.5 μm , which were corresponding to those obtained by LCM observation. The size of colloidal crystals formed from polymer-modified silica in organic solvents was generally small less than several dozens of μm . However, Okubo [37] reported that colloidal crystals of silica or polymer latexes in aqueous solution increased grew in 4-5 mm size, of which decreased with particle volume fraction. The reason why small size crystals formed in organic solvent as compared with those in water probably comes from lower polarity of the solvent. Higher particle volume fraction probably led to formation of much number of crystallites to give small crystals. It was also observed that the crystal sizes were observed to be inclined to decrease during two-step polymerization. Actually, intensity of reflection peak drastically decreased after gelation probably due to destruction or decrease of number of the crystals.

Table 1. Single crystal size of colloidal crystals

ϕ	Size (L) / μm	
	Solution ^{a)}	Gel ^{b)}
0.11	18.8 \pm 2.3 (13.8[5.6])	13.9 [5.6]
0.14	14.7 \pm 2.0 (6.7[1.8])	3.3 [1.7]
0.18	5.5 \pm 1.3 (4.6[1.3])	7.5 [1.7]

a) Determined by Eq. (4). Values in parentheses are ones estimated by LCM observation along with standard deviation in brackets.

b) Determined by LCM observation. Values in brackets are standard deviation.

3.3.4 Inter-sphere distance

Inter-sphere distance (d_{obs}) between neighboring particles in acetonitrile at $\phi = 0.11, 0.14,$ and $0.18,$ gel and PMMA matrix estimated by Bragg's equation using reflection peak wave length are listed in Table 2, along with the values (d_{calcd}) calculated by volume fraction of the particles on assumption of face-centered cubic(FCC) closed packing. The observed distances in colloidal crystals formed in acetonitrile decreased with increasing of ϕ and were coincident with calculated values, $d_{calcd},$ from volume fraction of the particles. These results suggested that colloidal crystals of PMMA-grafted silica were formed by FCC closed packing. The inter-sphere distances (d_{SEM}) in PMMA matrix were determined by SEM images of cross-section of PMMA matrix after etching. The distances, $d_{SEM}=258, 238,$ and 222 nm at $\phi=0.11, 0.14,$ and $0.18,$ respectively, in the matrix were fairly agreed with the values of those in colloidal crystals in acetonitrile. Therefore, these results indicated that the inter-sphere distances scarcely changed through two-step immobilization by radical polymerization, despite of much changing with swelling extent after gelation. Standard deviations of d_{SEM} at $\phi=0.11, 0.14,$ and 0.18 were $30, 16,$ and 12 nm at $\phi=0.11, 0.14,$ and $0.18,$ respectively, which were corresponding to $11.6, 6.7,$ and 5.4% of respective inter-sphere distance (Table 2). Thus, immobilization of colloidal silica formed in solution made much disordering of particle array at lower particle volume fraction. At higher volume fraction than $0.2,$ however, colloidal crystallization of PMMA-grafted silica in acetonitrile was never observed, probably due to relatively high interaction between PMMA chains grafted on silica to disturb electric repulsion between the particles (figure 5).

Table 2. Inter-sphere distance in colloidal crystals in solution, gel and PMMA matrix

ϕ	Inter-sphere distance / nm				
	Solution		Gel	Solid	
	d_{calcd}	d_{obs}	d_{obs}	d_{obs}	$d_{SEM}^{a)}$
0.11	264	257	265	279	258 [30]
0.14	253	242	275	240	238 [16]
0.18	232	222	224	217	222[12]

a) Values in parentheses are standard deviation in nm.

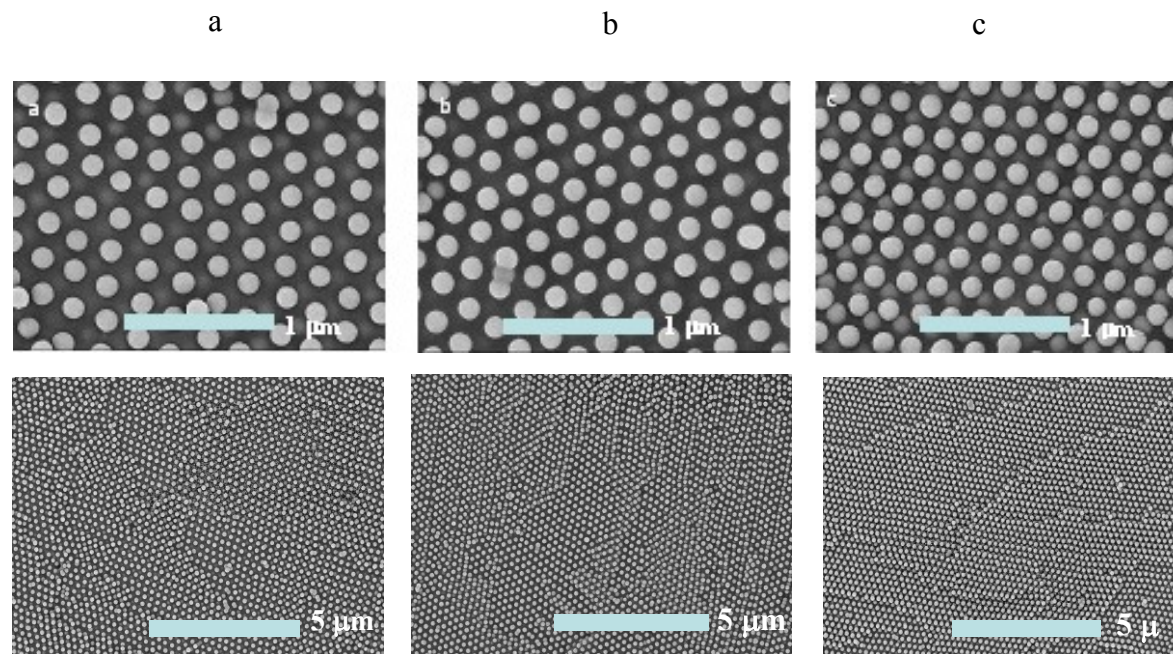


Figure 5. Cross-sectional SEM images of colloidal crystals-immobilized PMMA matrix; a, b, and c are at $\phi=0.11$, 0.14, and 0.18, respectively.

3.4 Conclusions

Effects of particle volume fraction on distortion in particle-arrayed structure in colloidal crystals formed by PMMA-grafted silica in acetonitrile through immobilization by two-step polymerization were investigated. Crystal sizes in colloidal crystals in solution were independent on particle volume fraction in the range 0.11-0.18, but the size and number of the crystals decreased during gelation. It was also observed that inter-sphere distances in colloidal crystals were preserved during the immobilization. Disordering in particle-arrayed structure in colloidal crystals formed at higher volume fraction, $\phi=0.18$, was observed to be relatively low through two-step polymerization. These results showed that immobilization of colloidal crystals formed in higher volume fraction, i.e. under circumstance of high electrostatic repulsion, led to preservation of low disordering in particle array with the standard deviation within 5.4% of the inter-sphere distance during two-step polymerization.

3.5 References

1. Holtz, J.H.; Asher, S.A.; *Nature* 1997, 389, 829.
2. Lee, K.; Asher, S.A.; *J. Am. Chem. Soc* 2000, 122, 9534.
3. Reese, C.E.; Mikhonin, A.V.; Kamenjicki, M.; Tikhonov, A.; Asher, S.A.; *J. Am. Chem. Soc* 2004, 126, 1493.
4. Muscatello, M.M.W.; Stunja, L.E.; Asher, S.A.; *Anal. Chem* 2009, 81, 4978.
5. Xia, Y.; Gates, B.; Yin, Y.; Lu, Y.; *Adv. Mater* 2000, 12, 693.
6. Muscatello, M.M.W.; Stunja, L.E.; Thareja, P.; Wang, L.; Bohn, J.J.; Velankar, S.S.; Asher, S.A.; *Macromolecules* 2009, 21, 44037.
7. Cong, H.; Cao, W.; *Langmuir* 2004, 20, 8049.
8. Park, J.H.; Ohoi, W.S.; Koo, H.Y.; Kim, D.Y.; *Adv. Mater* 2005, 17, 879.
9. Kuai, S.L.; Bader, G.; Ashrit, P.V.; *Appl. Phys. Lett* 2005, 86, 22110.
10. Jiang, P.; Bertone, J.F.; Hwang, K.S.; Colvin, V.L.; *Chem. Mater* 1999, 11, 2132.
11. Lyon, A.L.; Debord, J.D.; Debord, S.B.; Jones, C.D.; McGrath, J.G.; Serpe, M.J.; *J. Phys. Chem. B* 2004, 108, 19099.
12. Fudouzi, H.; Xia, Y.; *Langmuir* 2003, 19, 9653.
13. Camargo, P.H.; Lee, Y.H.; Jeong, U.; Zou, Z.; Xia, Y.; *Langmuir* 2007, 23, 2985.
14. Nakamura, H.; Ishii, M.; Tsukigase, A.; Harada, M.; Nakano, H.; *Langmuir* 2006, 22, 1268.
15. Ishii, M.; Nakamura, H.; Nakano, H.; Tsukigase, A.; Harada, M.; *Langmuir* 2005, 21, 5367.
16. Nakamura, H.; Shii, M.; Tsukigase, A.; Harada, M.; Nakano, H.; *Langmuir* 2005, 21, 8918.
17. Nakamura, H.; Ishii, M.; *Langmuir* 2005, 21, 11578.
18. Nakamura, H.; Mitsuoka, T.; Ishii, M.; *J. Appl. Polym. Sci* 2006, 102, 2308.
19. Takeoka, Y.; Watanabe, M.; *Langmuir* 2003, 19, 9554.
20. Kumada, M.; Watanabe, M.; Takeoka, Y.; *Langmuir* 2006, 22, 4403.
21. Sakai, T.; Takeoka, Y.; Seki, T.; Yoshida, R.; *Langmuir* 2007, 23, 8651.

22. Sawada, T.; Suzuki, Y.; Toyotama, A.; Iyi, N.; *Jpn. J. Appl. Phys* 2001, 40, 1226.
23. Yamanaka, J.; Murai, M.; Iwayama, Y.; Yonese, M.; Ito, K.; Sawada, T.; *J. Am. Chem. Soc* 2004, 126, 7156.
24. Toyotama, A.; Yamanaka, J.; Shinohara, M.; Onda, S.; Sawada, T.; Yonese, M.; Uchida, F.; *Langmuir* 2009, 25, 589.
25. Evanoff, D.D.; Hayes, S.E.; Ying, Y.; Shim, G.H.; Carroll, L.J.R.; Houchins, J. M.; Huebner, C.F.; Foulger, S.H.; *Adv. Mater* 2009, 19, 3507.
26. Okubo, T.; *Acc. Chem* 1986, 82, 3163.
27. Okubo, T.; *Colloid. Surf. A* 1996, 109, 97.
28. Yoshinaga, K.; Shigeta, M.; Komune, S.; Mouri, E.; Nakai, A.; *Colloids and Surfaces B: Biointerfaces* 2007, 54, 10.
29. Yoshinaga, K.; Chiyoda, M.; Yoneda, A.; Nishida, H.; Komatsu, M.; *Colloid. Polym. Sci* 1999, 28, 481.
30. Yoshinaga, K.; Chiyoda, M.; Ishiki, H.; Okubo, T.; *Colloid. Surf. A* 2002, 204, 285.
31. Yoshinaga, K.; Fujiwara, K.; Tanaka, Y.; Nakanishi, M.; Takesue, M.; *Chem. Lett* 2003, 32, 1082.
32. Yoshinaga, K.; Fujiwara, K.; Mouri, E.; Ishii, M.; Nakamura, H.; *Langmuir* 2005, 21, 4471.
33. Yoshinaga, K.; Mouri, E.; Ogawa, J.; Nakai, A.; Ishii, M.; Nakamura, H.; *Colloid. Polym. Sci* 2004, 283, 340.
34. Yoshinaga, K.; Nakanishi, K.; *Compos. Interf* 1994, 2, 95.
35. Okubo, T.; Okada, S.J.; *Colloid. Interface. Sci* 1998, 204, 198.
36. Okubo, T.J.; *Chem. Soc, Faraday. Trans* 1986, 182, 3163.
37. Okubo, T.; *Colloid, Surf, A* 1996, 109, 77.

Conclusion

Colloidal silica modified with copolymer tethering ferrocenyl group, poly(FcMA-co-MMA) and poly(FcMA-block-MMA), brought colloidal crystallization in DMF and acetonitrile. Normalized effective refractive index by volume fraction of the particles increased with mole fraction of FcMA in copolymer. The introduction of ferrocenyl group into grafted copolymer led to enlargement of refractive index of colloidal silica systems.

Effects of particle volume fraction on distortion in particle- arrayed structure in colloidal crystals were investigated. Crystal sizes and number in crystals decreased during gelation and inter-sphere distances in colloidal crystals were preserved during the immobilization. Disordering in particle-arrayed structure in colloidal crystals formed at higher volume fraction, $\phi=0.18$, was observed to be relatively low through two-step polymerization.

Acknowledgements

I greatly appreciate Professor Kohji Yoshinaga at the Department of Materials Science, Graduate School of Engineering, Kyushu Institute of Technology for giving me the opportunity to engage in this study, guidance, and valuable suggestion throughout this work. I express sincerely my thanks to Professor Akihiko Tsuge, Seishi Takaki, Teruhisa Ohno and Associate Professor Toshiki Tsubota for their valuable suggestion and helpful advice. I also wish to express my sincerest gratitude to Assistant Professor Emiko Mouri, Mr. Shuhei Yamada, Dr. Zhifeng Wang, Mr. Mahiro Nakano, Mr. Seishu Komune, Mr. Ryosuke Koga, Miss. Miwa Watanabe and all the members of Yoshinaga's lab for helpful suggestions and hearty encouragement.

Furthermore, I wish to express his deep appreciation to my parents, Mr. Pu MA, and Mrs. XiuLian DU for their continuous assistance and warm encouragement.

ZhiGuo MA

Department of Materials Science
Graduate School of Engineering
Kyushu Institute of Technology
March, 2011

Publication list

1. Effects of ferrocenyl group on refractive index of colloidal crystal system formed by polymer-grafted silica in organic solvent, ZG Ma, M Watanabe, E Mouri, K Yoshinaga (2010) *Colloid Polym Sci* 288:519
2. Effects of particle volume fraction on distortion of particle-arrayed structure during immobilization of colloidal crystals formed by poly(methylmethacrylate)-grafted silica in acetonitrile, ZG Ma, M Watanabe, E Mouri, A Nakai, K Yoshinaga (2011) *Colloid Polym Sci* 289:85